Investigating the role of calcium ion mobilization in NLRP3 inflammasome activation of J774A.1 macrophages and optimizing cell morphology and IL-1β quantification protocols

Parneet Sekhon, Rajeshwar Singh, Andrew Song

Department of Microbiology and Immunology, University of British Columbia, Vancouver, British Columbia, Canada

SUMMARY The nucleotide-binding domain, leucine-rich-repeat-containing family, pyrin domain-containing 3 (NLRP3) inflammasome is responsible for sensing and regulating the inflammatory response. When activated, NLRP3 inflammasomes can upregulate inflammatory cytokines such as IL-1β and IL-18, which are often associated with changes in cell morphology and can lead to pyroptosis. NLRP3 activation is also regulated by several upstream events such as calcium mobilization, but explicit mechanisms of activation have yet to be resolved. To investigate the effect of calcium mobilization on NLRP3 activation, we quantified changes in cell morphology and IL-1β release in response to LPS and ATP. LPS-primed J774A.1 cells were stimulated with 5mM or 2mM ATP for various lengths of time, and we used phase-contrast microscopy to visualize cell morphology changes as well as protein-based assays to quantify IL-1β release. We observed cell morphology changes in response to stimulation, and areas for troubleshooting and further optimization were identified for these methods of quantification. However, we were not able to detect the release of cleaved IL-1β. Future studies could explore more suitable conditions for LPS and ATP stimulation and formally investigate the role of calcium in inflammasome activation.

INTRODUCTION

Inflammasomes are multi-protein complexes that are important sensors and regulators of the inflammatory response. They can be activated by a large variety of signals, including pathogen-associated molecular patterns (PAMPs, such as viral RNA or bacteria) or damage-associated molecular patterns (DAMPs, such as ion flux, mitochondrial dysfunction, and lysosomal disruption). They can also sense crystalline substances such as alum, silica and endogenous danger signals like ATP (1–3). The NLRP3 (nucleotide-binding domain, leucine-rich-repeat-containing family, pyrin domain-containing 3) inflammasome is particularly critical for defense against bacterial, fungal and viral infections (4). It consists of the regulatory subunit NLRP3, the adaptor protein known as apoptosis-associated speck-like protein containing a caspase-recruitment domain (ASC), and the effector subunit caspase-1 (5). Activation of inflammasomes in response to one or more stimulants leads to cleavage of an enzyme called procaspase-1 into its active caspase-1 form. Caspase-1 then proceeds to cleave inflammatory cytokines pro-IL-1β and pro-IL-18 into their active forms, IL-1β and IL-18, respectively (1). In addition, caspase-1 also cleaves gasdermin D (GSDMD), causing it to migrate to the cell membrane and form pores through which IL-1β and IL-18 are released (6). The release of these cytokines induces the inflammatory death known as pyroptosis. However, dysregulation of the NLRP3 inflammasome has been shown to be linked to several disorders such as cryopyrin-associated periodic syndromes (CAPS), exacerbation of disease symptoms, Alzheimer's disease, diabetes, gout and atherosclerosis (1, 4). These findings further emphasize the critical role of inflammasomes and the need for further investigation of specific activation mechanisms.

Activation of the NLRP3 inflammasome is thought to include multiple upstream signaling events, such as the efflux of potassium (K+) and chloride ions (Cl-), mobilization of calcium ions (Ca2+), lysosomal disruption, mitochondrial dysfunction and metabolic changes (5, 7). In particular, Ca2+ mobilization controls diverse cellular processes, including proliferation and differentiation, transcription, cellular metabolism, and cell death (8). It has

been shown to be an important upstream event leading to NLRP3 inflammasome activation (5, 9). Mobilization of Ca2+ occurs by one of two pathways: the opening of channels in the plasma membrane to allow Ca2+ ions to enter the cytosol, or the release of endoplasmic reticulum (ER) stores of Ca2+ (7). Previous studies have shown that K+ efflux can act as an additional mediator of Ca2+ mobilization by acting as a counter-ion at the plasma membrane (10). Inflammasome activation can also be promoted by the release of ER stores of Ca2+ followed by a massive entry of extracellular Ca2+ by a process known as "store-operated calcium entry (SOCE) (5, 10). The most common method of investigating Ca2+ in inflammasome activation is through the use of inhibitors such as 2-aminoethoxy diphenylborinate (2-APB), which block SOCE, and measured inflammasome activation via IL-1β release (11). Previous studies showed that Ca2+ mobilization was necessary for inflammasome activation, since the inhibition of Ca2+ hindered IL-1β release and caspase-1 activation (5, 7, 10). Other studies have reported the contrary, that the NLRP3 inflammasome could be activated independently of Ca2+ (9, 12). Thus, the role of Ca2+ mobilization in NLRP3 inflammasome activation remains controversial, and further elucidation of these mechanisms is needed.

We aimed to investigate the effect of calcium ion mobilization on NLRP3 inflammasome activation by quantifying IL-1β release as well as general effects on cell morphology and health. Since LPS and/or ATP stimulation was reported to induce common parts of the inflammasome activation pathway such as morphological changes, calcium influx and apoptosis (13–17), we hypothesized that stimulation of murine macrophages would lead to similar effects.

We studied conditions that elicited the greatest response to LPS and ATP by quantifying cell morphology changes and attempted to quantify IL-1β release. In addition, we used the calcium channel inhibitor 2-APB to see the effect of calcium deficiency on IL-1β release and cell morphology. Although we were not able to provide conclusive evidence regarding the effect of Ca2+, potential measures of morphology and IL-1β quantification were piloted, giving future researchers the opportunity to refine and advance protocols to elucidate the mechanisms for inflammasome activation.

METHODS AND MATERIALS

Cell culture. The J774A.1 mouse macrophages (Kronstad Lab, Michael Smith Laboratories, UBC) were cultured in high glucose- Dulbecco's Modified Eagle Medium (DMEM) and supplemented with 10% fetal bovine serum and 2mM L-glutamine (ThermoFisher Scientific, 25030-081). The cells were grown in an incubator with 5% CO2 at 37 °C. Every 2 or 3 days, the cultures were expanded for use in experiments or maintenance in culture until a passage number of five was reached. For western blot experiments, cells were seeded in 6-well plates at a density of 100,000 cells/mL, and 2mL of cell suspension was added to each well. For ELISA, cells were seeded in a 24-well plate at a density of 50,000 cells/mL, and 1mL of cell suspension was added to each well (see Supplemental Figure 2).

Reagent preparation. A 1mg/mL stock solution of LPS (Sigma-Aldrich, L4391) was diluted to make 500ng/mL aliquots of LPS. During priming steps, this new stock solution was diluted in DMEMc to reach a final concentration of 50ng/mL before adding to each well. ATP (Sigma-Aldrich, A2383-1G) was dissolved in PBS to make stock aliquots at 25mg/mL and pH was neutralized by addition of sodium hydroxide (NaOH). 2-APB (Millipore Sigma, D9754) was dissolved in DMSO to make a stock solution of 25mg/mL. All diluted stock solutions were stored at -20°C throughout the experiments and thawed before use. 1x RIPA lysis buffer was prepared for protein extraction by mixing 50mM Tris (pH 7.5), 150mM NaCl, 1% NP-40, 0.5% sodium deoxycholate, and 0.1% sodium dodecyl sulfate (SDS).

SDS-PAGE and western blot. Total proteins from J774A.1 cells were extracted using a protease inhibitor tablet (Roche, 11697498001) dissolved in 1x RIPA buffer. Protein concentration was measured using a BCA Protein Assay Kit (ThermoFisher, 23225). Equal amounts of protein (20 μg) were separated by SDS-polyacrylamide gel electrophoresis (PAGE) at 120V and transferred onto a PVDF membrane overnight at 20V. The membrane

was then blocked with 5% skim milk in TBS-T for 1 hour at room temperature. Next, membranes were incubated with a goat anti-mouse IL-1β primary antibody (R&D, AF-401-SP) att 1:1000 dilution at 4 °C overnight. After rinsing the membranes with TBST-T 3 times for 5 minutes each, the membranes were incubated with the anti-goat HRP secondary antibody (Jackson ImmunoResearch, 305-035-003) diluted at 1:15000 in 1% skim milk for 45 minutes at room temperature. The protein bands were visualized by ECL reagent (ThermoFisher, 32106) in the BioRad ChemiDoc MP Imager. The densities of the bands were assessed by GraphPad (Prism) software.

ELISA. An IL-1β mouse ELISA kit (ThermoFisher, 88-7013-86) was used to conduct the assay and the following steps were performed according to the manufacturer's instructions. All wells in a 96-well plate were coated overnight with 100uL each of 1x PBS. The next day, PBS was aspirated from the wells and wash buffer (>250uL) was added to rinse the wells 3 times for a few minutes each. Then, 200uL of 1X ELISA/ELISPOT diluent was added to each well for blocking and the plate was incubated for 1 hour at room temperature. The wells were then rinsed again with wash buffer 100uL/well of samples were added to the appropriate wells. The plate was sealed with parafilm and incubated at 4°C for 4 hours. The wells were aspirated and rinsed with wash buffer, and blotted on absorbent paper to remove any residual buffer. Next, 100uL of the detection antibody was added to all wells, after which the plate was sealed and incubated for 1 hour at room temperature. After aspirating the antibody solution and rinsing with wash buffer, 100uL of diluted HRP enzyme solution was added to each well. The plate was again sealed and incubated for 30 minutes at room temperature. The wells were again aspirated and rinsed with wash buffer, and 100uL of 1X TMP solution was added to each well. After a 15 minute incubation at room temperature, 100uL of stop solution was added to each well. The 96-well plate was then read at 450 nm using a microplate reader.

Cell Imaging. The cells were observed using the primovert inverted phase contrast microscope fitted with a camera (Axiocam ERc5s) at 40x magnification. Images were taken at different timepoints: before LPS stimulation, post 24 hour LPS stimulation, as well as after 1 hour, 2 hour, 4 hour, or 24 hour of stimulation with ATP.

Image Analysis. Image processing and quantification of cell morphologies was done using the ImageJ software. For quantification of cell morphology changes, cells were chosen in a semi-random fashion; 4 cells were randomly selected from each corner and one was randomly selected in the center. The cell were then outlined and their measurements recorded. For the western blot, the peak intensities were measured and peak areas were approximated.

RESULTS

Pro-Il-1β production increases, but no detection of cleaved Il-1β in response to cell stimulation with LPS and ATP

In order to understand whether calcium deficient cells have decreased inflammasome activation, we first characterized the normal inflammasome response in J774A.1 cell lines. To this end, we performed a western blot probing for IL-1β after stimulating LPS-primed J774A.1 cells with ATP or nigericin. Calcium free conditions were also included by using regular DMEMc or PBS media.

There is distinct pro-IL-1β production in stimulated cells as compared to the unstimulated cells, but no cleavage product characteristic of NLRP3 inflammasome activation (Fig.1A). In the conditions lacking calcium, a faint lower band can be observed indicating potential cleavage products. Interestingly, this does not support the hypothesis that calcium is required for inflammasome activation. These results also indicate that the quantity of pro-IL-1β between the conditions does not considerably vary. Observation of the faint, secondary bands led us to perform an ELISA to see if we can quantify the cleaved IL-1β and find any differences between conditions. However, the results showed little to no detection of IL-1β except for select conditions whose fold change was shown (see Supplemental Figure 1). The low detection could be a result of a technical error in ELISA or a technical error in the stimulation. In the stimulation, the issue could be with the LPS which is used for priming, or ATP which is used for the second signal.
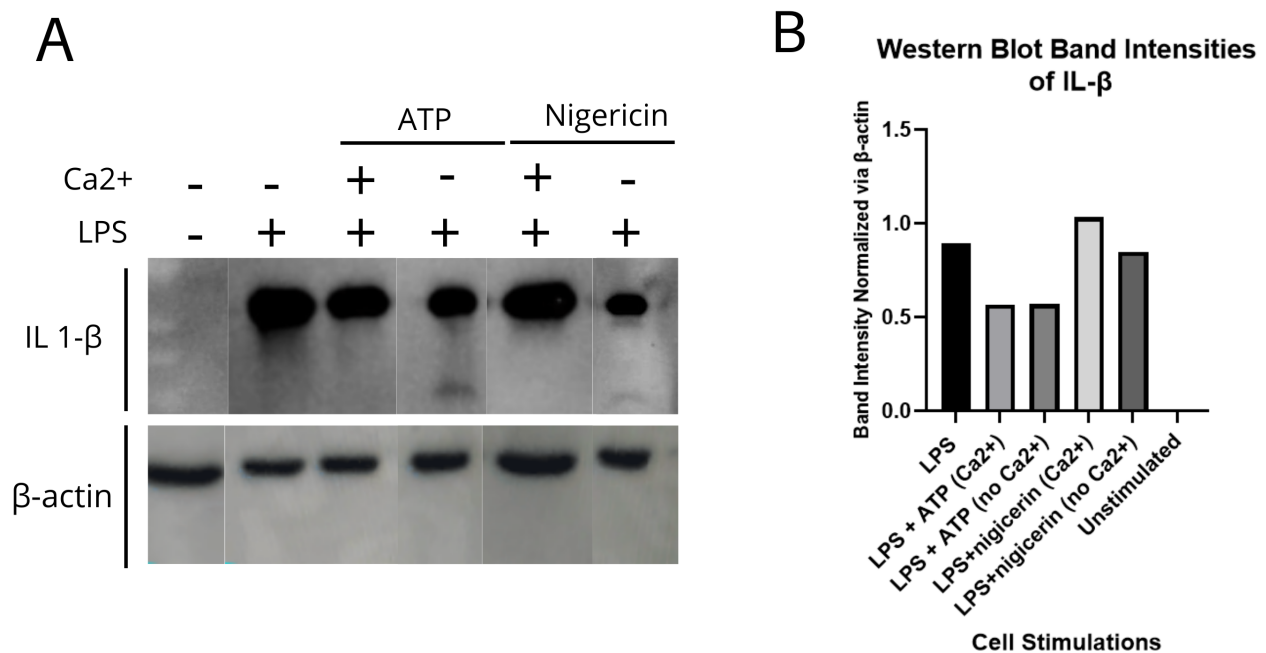
FIG. 1 LPS exposure coupled with ATP and nigericin leads to an increase in pro-IL-1β production compared to completely unstimulated cells. (A) Western blot bands probing for IL-1β from 15µg of J774A.1 cell lysates stimulated under the following conditions; LPS, LPS + ATP + DMEM, LPS + ATP + PBS, LPS + Nigericin + DMEM, LPS + nigericin + PBS. The stimulation times were as follows: (LPS) 24 hr, (ATP) 30 min, (Nigericin) 1 hr. (B) Chara cauterization of the beta-actin-normalized band intensities, using ImageJ software, indicates similar intensities between stimulation conditions.

Cell perimeter and circularity change in response to a 24hr LPS stimulation.

Having failed to see cleaved IL-1β, it was unknown whether these results were due to an error in the ELISA or the stimulation. To investigate potential causes behind these results, an LPS time course was done to visualize the morphological changes (Area, Perimeter, Circularity) due to the initial LPS stimulation.

After LPS stimulation, typically a morphological change takes place as a result of F-actin cytoskeleton rearrangements (16). Visually, our results did not show a considerable degree of morphological difference. Images were taken of cells before and after 24hrs of LPS stimulation (Fig. 2A). On observation alone, the 24 hour stimulated cells appear round and healthy with minimal discernible differences from the unstimulated cells, which is contrary to our hypothesis (Fig. 2A). This is corroborated by the minimal change in cell area (Fig. 2B) which stands as a rough substitute for cell volume. The variation between cell density in the two photos can be accounted for by differences of the photo location with the well. When quantifying the perimeter and circularity (Fig.2B, Fig.2C), we found that perimeter increased while circularity of the cells decreased across most biological replicate conditions. These quantifications of perimeter and circularity suggest that the changes observed are due to cell shape changes and not cell volume changes and this is indicative of successful stimulation.

J774A.1 cells exhibit an increase in cell death when stimulated with 5mM ATP for a 24 hour period.

After our initial pilot experiment with LPS-primed cells, we continued to study signal 2 of inflammasome activation via ATP stimulation. Various concentrations and times of ATP stimulation were tested to optimize for inflammasome activation through visualization of cell morphological changes.

When analyzing the images (Fig. 3A), five cells were chosen at random, which were then outlined using ImageJ. Cell area, perimeter and circularity were quantified similarly as in Figure 2. The microscope images also had a scale bar which was used to convert the pixel distance to micrometers. There was a visible decrease in cell confluency and
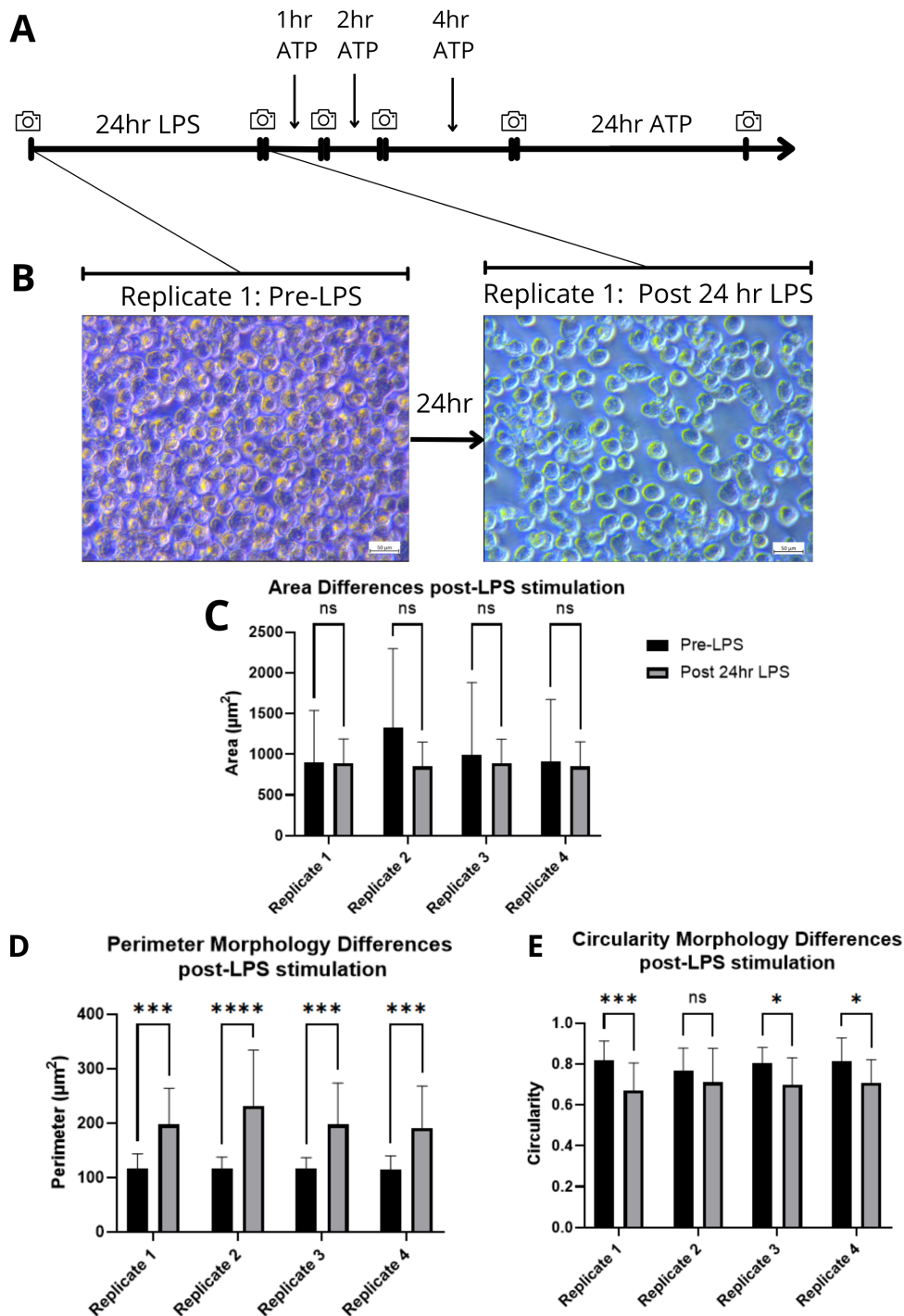
FIG. 2 LPS stimulation of J774A.1 cells for 24hr led to an increase in perimeter length and a decrease in circularity. (A) Time course of cells and showing the time points at which images were taken. There were 4 biological replicates of cells with 4 technical replicates each (B) Images of pre- and post-24hr LPS stimulation conditions for one biological replicate. Images were taken with the Zeiss ERc5s monochrome camera at 40X magnification. Scale bar represents 50μm. (C) 5 cells per condition were chosen at random and their respective area was measured before and after stimulation using ImageJ. The results indicate no significant change of the between the areas at the two time points. (D) Using the 5 randomized cell selection approach for measuring perimeter, significant increases were noticed in each condition within the two time points. 24hr LPS stimulation resulted in increased perimeters. The p-values from a two- way ANOVA are as follows from left to right; 0.0002(***), 0.0001 (****), 0.0002(***), 0.0003 (***). (D) Same 5 cell randomized selection criteria as before, however the circularity of cells was calculated. An overall decrease was seen in circularity with the p-values from a two-way ANOVA as follows from left to right; 0.0008 (***), 0.3942 (ns), 0.0232(*), 0.0219(*).

distortion of morphology beginning at the 4 hour mark and was most severe at the 24 hour mark (Fig. 3A).
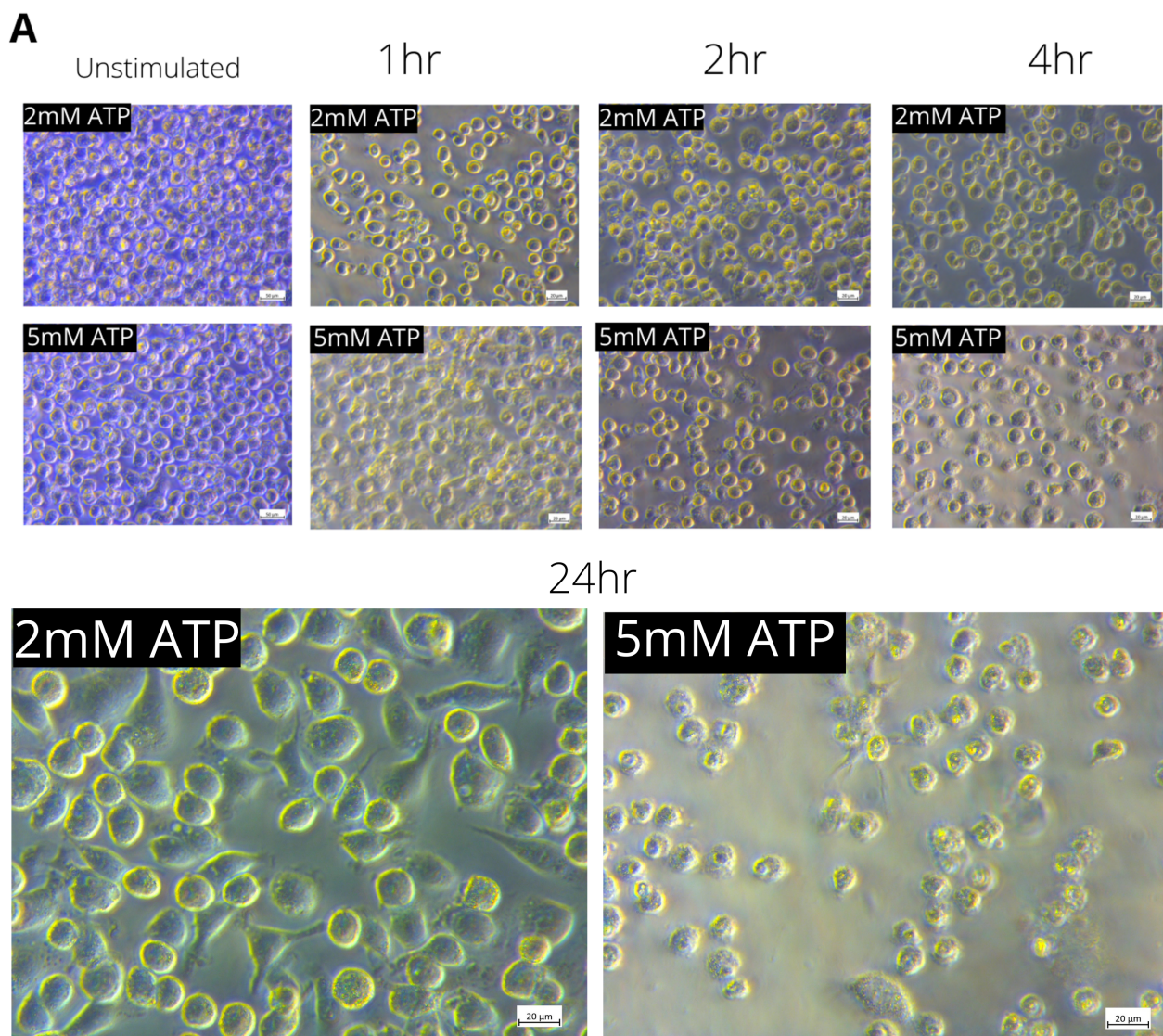

FIG. 3 J774A.1 murine macrophages die after 4hr and 24hr in 5mM ATP conditions and show increased death compared to the 2mM ATP condition. (A) Images were taken at 40X magnification using the Zeiss ERc5s monochrome camera. Scale bar represents 50μm. Each column represents the treatment conditions of a biological replicate which was photographed after 1hr, 2hr, 4hr or 24hr of ATP stimulation.

When the 2-APB inhibitor was added to the LPS-primed cells prior to the ATP stimulation, we observed a decrease in cell confluency with 5mM ATP compared to 2mM ATP in the 4 hour stimulation period, even in the presence of 2-APB (Fig. 4A). Interestingly, we observed a distortion of cell shape in the 2mM ATP condition when LPS-primed cells were stimulated with ATP for 24 hours, whereas the cells in the corresponding 5mM ATP condition appeared spherical and healthy in the presence of 2-APB (Fig. 4A). Therefore, these results suggest that 5mM ATP stimulation for 4 hours induces the most change in cell area and perimeter, and is also affected by the presence of 2-APB. Thus, it may be the best stimulation condition for future experiments.
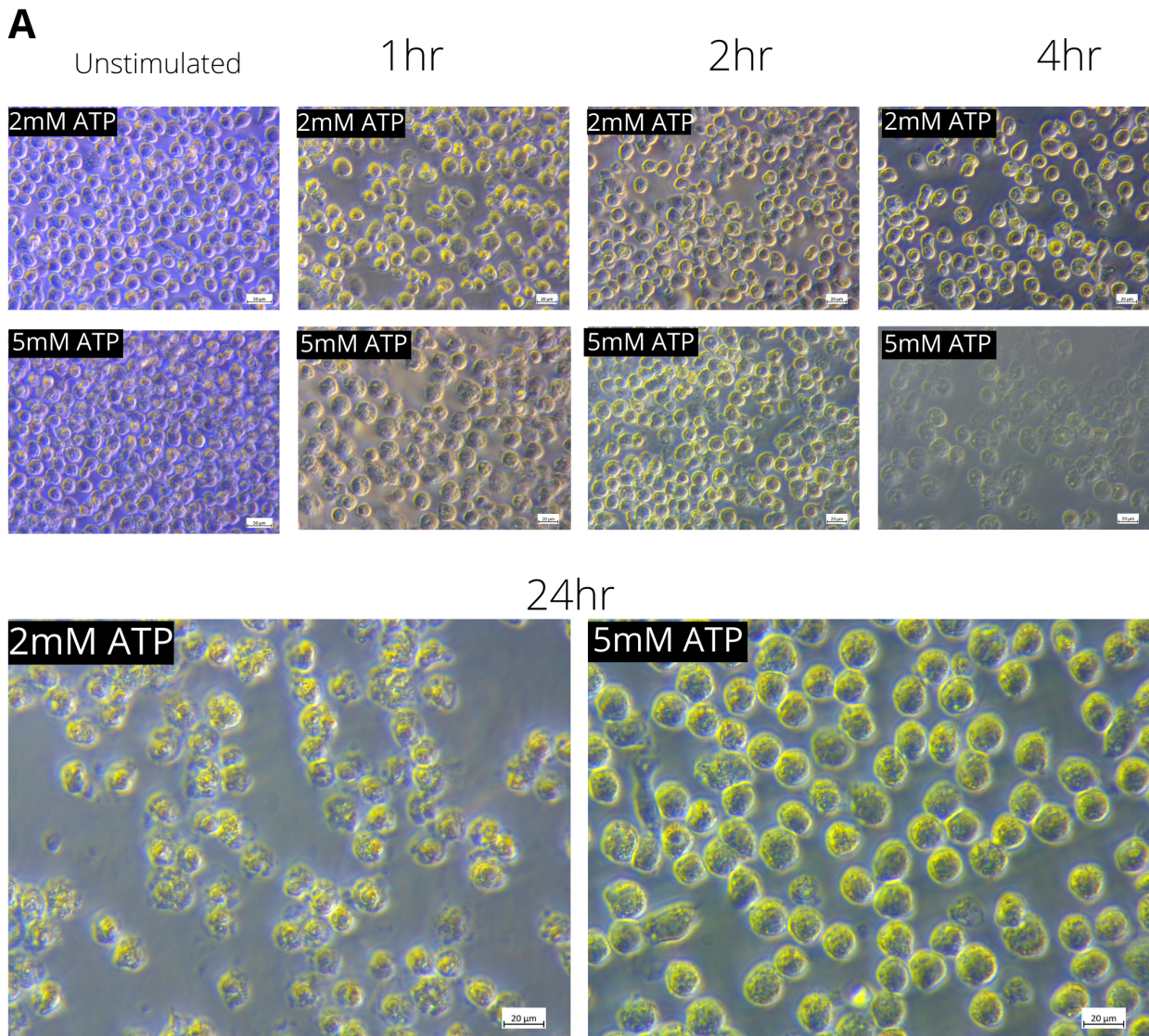
A

FIG. 4 J774A.1 murine cells show death at 4hr and 24hr ATP stimulation even in the presence of 2-APB. (A) Images were taken at 40X magnification using the Zeiss ERc5s monochrome camera. Scale bar represents 50μm. Each column represents the treatment conditions of a biological replicate which was photographed after 1hr, 2hr, 4hr or 24hr of ATP stimulation with 2-APB added.

DISCUSSION

In this paper, we have demonstrated potential methods to be used for studying NLRP3 inflammasome activation. We have further shown that cells stimulated with ATP show a significant increase in their perimeter compared to their pre-ATP counterparts. Using different timepoints to visualize cell morphology changes post-ATP stimulation, we were able to develop the basis of an experimental design for studying NLRP3 inflammasome activation. However, we were not able to observe IL-1β cleavage in our western blot results and we did not detect a significant level of IL-1β protein in our quantitative analysis using ELISA.

Overall, our results were not conducive to our hypothesis. Originally, we wanted to understand the dynamics of calcium mobilization and its role in activating the NLRP3 inflammasome. However, we first needed to activate the NLRP3 inflammasome but we failed to see adequate cleavage of IL-1β, a protein activated during the pathway (Fig.1). The only cleavage observed (Fig.1.A) was in the calcium free conditions, contrary to our hypothesis.

Additionally, it is still unclear whether the cleaved products seen are truly IL-1β products as our ladder was not distinct enough to provide accurate size references for the additional bands. Secondary attempts of the western blot were made to account for technical error but they did not provide any useful results. We also attempted an ELISA to quantify the secreted IL-1β yet we did not attain any meaningful results. Thus, we decided to take an in-depth look into the LPS priming and ATP stimulation.

We also failed to see morphological changes associated with LPS stimulation (Fig.2). According to literature, the LPS stimulation results in drastic cellular changes; filopodia and lamellipodia formation and extension (15). These morphologies are due to F-actin cytoskeleton remodeling and can usually be seen within 3 hours (16). However, at our 24-hour stimulation mark, our cells were fairly rounded and healthy looking with little to no discernable morphological change. Nakamura et al. (1999) suggest that after a certain time point, LPS stimulated cells revert from the bipolar/ tripolar shapes to circular cells smaller in area than unstimulated cells. It is possible that we missed out on the time point where the cell morphology would be drastically different. However it seems unlikely that all cells would revert back to a rounded shape and the literature also suggests the 24 hour LPS primed cells have a smaller area than the control cells whereas our cells had negligible size differences. Our investigation here helped us understand the primary issue with our cells was the initial LPS priming which can likely account for the lack of IL-1β in the ELISA (see Supplemental Figure 1). To account if our cells are failing to respond to LPS, the cells should be imaged more frequently at different time points during LPS stimulation. A western blot to detect caspase-1 protein would also show whether cleavage products are being produced as a result of LPS priming. In future experiments, cells passaged a fewer number of times should be utilized to prevent passage-based alterations and unintended morphological changes in cells. It is suggested that working cultures should have an average max passage number of 5 while we used J774A.1 cells that were passaged 6 times. Increasing passage numbers can result in genetic drift as well as alterations to key functions of the cell which in our case could cause a lack of priming in response to LPS (18).

Our results indicate an issue with LPS stimulation, as observed by a lack of morphological changes. Literature suggests that even after 4 hours post LPS, a discernible change in morphology can be seen. The formation of lamellipodia and dendrite-like extensions is usually observed and this corresponds to an increase in perimeter and decrease in circularity measurements. However in our case, none of those were observed with the cells maintaining a circular shape post 24 hr LPS stimulation. It is possible that our working LPS concentration of 50ng/mL was not enough to effectively stimulate the J774A.1 P5 cells; importantly, stimulation with 100ng/mL LPS or 1ug/mL of LPS have resulted in drastic changes in cell morphology (11, 14).

Furthemore, due to technical issues with loading our samples onto the gel in preparation for the western blot, there was some spillage across the wells. The bands of the ladder were also not discrete enough for us to effectively quantify the relative size of the bands observed. It is possible that the lack of cleavage observed was also in part due to an insufficient amount of protein loaded onto the gel. Considering that the "calcium-free" conditions utilized PBS as a culture medium, the lack of nutrients and growth factors would have prevented cells from adhering properly to the well, thus reducing the amount of protein that could be extracted. Future experiments using a calcium-free, nutrient-rich medium may be beneficial in extracting more protein from plated wells.

When cells are exposed to extracellular ATP, it acts as an additional stimulant in the NLRP3 inflammasome activation pathway leading up to pyroptosis. Pyroptosis is similar to apoptosis in regards to the observable features of the processes. These morphological features include; nuclear condensation, plasma membrane pore formation, cellular swelling, rupture (19). When looking at the time course images (Fig.3A, Fig.4A), cellular debris and apoptotic cells become visible in the later time points; 5mM ATP at 4hr mark, 5mM ATP + 2-APB. However, for the 2mM timepoints, some cells exhibit a bipolar morphology characteristic of LPS stimulation. An attempt was made to quantify the morphological changes overtime, but the addition of cell debris and cell death to these results added variance and made it difficult to observe a trend.

Conclusions In conclusion, this study attempted to optimize methods to quantify NLRP3 inflammasome activation (via cell morphology and IL-1β release) in response to LPS and ATP stimulation, both with and without calcium present. Although the findings were inconclusive with regard to the effect of calcium, we were able to shed light on opportunities for troubleshooting to improve the reliability of these methods. Future studies could be done to further elucidate the optimal conditions required for effective cell stimulation using LPS and ATP. With sufficient troubleshooting using this study as a baseline, researchers could also begin to look more closely at the effect of calcium deprivation through the use of 2-APB or other methods (such as the use of calcium-free media).

ACKNOWLEDGEMENTS

CONTRIBUTIONS

All authors contributed to laboratory experiments and data collection. All members conducted background research. A.S. was responsible for writing the abstract, introduction, supplemental figures and contributed to writing the methods, results and discussion sections. R.S. was responsible for data analysis and figure generation, as well as writing the results and discussion sections. P.S. was responsible for writing the materials and methods, supplemental material and contributed to the abstract, introduction, results and discussion sections.

REFERENCES

1. Vanaja, S. K., V. A. K. Rathinam, and K. A. Fitzgerald. 2015. Mechanisms of inflammasome activation: recent advances and novel insights. Trends in Cell Biology 25: 308–315.
2. Eisenbarth, S. C., O. R. Colegio, W. O'Connor, F. S. Sutterwala, and R. A. Flavell. 2008. Crucial role for the Nalp3 inflammasome in the immunostimulatory properties of aluminium adjuvants. Nature 453: 1122–1126.
3. Mariathasan, S., D. S. Weiss, K. Newton, J. McBride, K. O'Rourke, M. Roose-Girma, W. P. Lee, Y. Weinrauch, D. M. Monack, and V. M. Dixit. 2006. Cryopyrin activates the inflammasome in response to toxins and ATP. Nature 440: 228–232.
4. Kelley, N., D. Jeltema, Y. Duan, and Y. He. 2019. The NLRP3 Inflammasome: An Overview of Mechanisms of Activation and Regulation. Int J Mol Sci 20: 3328.
5. Murakami, T., J. Ockinger, J. Yu, V. Byles, A. McColl, A. M. Hofer, and T. Horng. 2012. Critical role for calcium mobilization in activation of the NLRP3 inflammasome. Proc Natl Acad Sci U S A 109: 11282–11287.
6. Huang, Y., W. Xu, and R. Zhou. 2021. NLRP3 inflammasome activation and cell death. Cell Mol Immunol 18: 2114–2127.
7. Swanson, K. V., M. Deng, and J. P.-Y. Ting. 2019. The NLRP3 inflammasome: molecular activation and regulation to therapeutics. Nat Rev Immunol 19: 477–489.
8. Clapham, D. E. 2007. Calcium Signaling. Cell 131: 1047–1058.
9. Gong, T., Y. Yang, T. Jin, W. Jiang, and R. Zhou. 2018. Orchestration of NLRP3 Inflammasome Activation by Ion Fluxes. Trends in Immunology 39: 393–406.
10. Yaron, J. R., S. Gangaraju, M. Y. Rao, X. Kong, L. Zhang, F. Su, Y. Tian, H. L. Glenn, and D. R. Meldrum. 2015. K+ regulates Ca2+ to drive inflammasome signaling: dynamic visualization of ion flux in live cells. Cell Death Dis 6: e1954.
11. Bootman, M. D., T. J. Collins, L. Mackenzie, H. L. Roderick, M. J. Berridge, and C. M. Peppiatt. 2002. 2-Aminoethoxydiphenyl borate (2-APB) is a reliable blocker of store-operated Ca2+ entry but an inconsistent inhibitor of InsP3-induced Ca2+ release. The FASEB Journal 16: 1145–1150.
12. Djillani, A., O. Nüße, and O. Dellis. 2014. Characterization of novel store-operated calcium entry effectors. Biochimica et Biophysica Acta (BBA) - Molecular Cell Research 1843: 2341–2347.
13. He, C., Y. Zhao, X. Jiang, X. Liang, L. Yin, Z. Yin, Y. Geng, Z. Zhong, X. Song, Y. Zou, L. Li, W. Zhang, and C. Lv. 2019. Protective effect of Ketone musk on LPS/ATP-induced pyroptosis in J774A.1 cells through suppressing NLRP3/GSDMD pathway. International Immunopharmacology 71: 328–335.

14. Souza, C. O., G. F. Santoro, V. R. Figliuolo, H. F. Nanini, H. S. P. de Souza, M. T. L. Castelo-Branco, A. A. Abalo, M. M. Paiva, C. M. L. M. Coutinho, and R. Coutinho-Silva. 2012. Extracellular ATP induces cell death in human intestinal epithelial cells. Biochimica et Biophysica Acta (BBA) - General Subjects 1820: 1867–1878.

15. Granstein, R. D., W. Ding, J. Huang, A. Holzer, R. L. Gallo, A. D. Nardo, and J. A. Wagner. 2005. Augmentation of Cutaneous Immune Responses by ATPγS: Purinergic Agonists Define a Novel Class of Immunologic Adjuvants. The Journal of Immunology 174: 7725–7731.

16. Nakamura, Y., Q. S. Si, and K. Kataoka. 1999. Lipopolysaccharide-induced microglial activation in culture: temporal profiles of morphological change and release of cytokines and nitric oxide. Neuroscience Research 35: 95–100.

17. Sheng, W., Y. Zong, A. Mohammad, D. Ajit, J. Cui, D. Han, J. L. Hamilton, A. Simonyi, A. Y. Sun, Z. Gu, J.-S. Hong, G. A. Weisman, and G. Y. Sun. 2011. Pro-inflammatory cytokines and lipopolysaccharide induce changes in cell morphology, and upregulation of ERK1/2, iNOS and sPLA2-IIA expression in astrocytes and microglia. Journal of Neuroinflammation 8: 121.

18. Abd-El-Basset, E., and S. Fedoroff. 1995. Effect of bacterial wall lipopolysaccharide (LPS) on morphology, motility, and cytoskeletal organization of microglia in cultures. Journal of Neuroscience Research 41: 222–237.

19. McClenahan, D., K. Hillenbrand, A. Kapur, D. Carlton, and C. Czuprynski. 2009. Effects of Extracellular ATP on Bovine Lung Endothelial and Epithelial Cell Monolayer Morphologies, Apoptoses, and Permeabilities. Clinical and Vaccine Immunology 16: 43–48.

20. Hughes, P., D. Marshall, Y. Reid, H. Parkes, and C. Gelber. 2007. The costs of using unauthenticated, over-passaged cell lines: how much more data do we need? BioTechniques 43: 575–586.

21. Jia, C., H. Chen, J. Zhang, K. Zhou, Y. Zhuge, C. Niu, J. Qiu, X. Rong, Z. Shi, J. Xiao, Y. Shi, and M. Chu. 2019. Role of pyroptosis in cardiovascular diseases. International Immunopharmacology 67: 311–318.